Structural and optical characterization of $Zn(OH)_2$ and its composites with graphite oxides

SM Z. Islam,[1,2] Taposh Gayen,[2] Alaa Moussawi,[2] Lingyan Shi,[3] Mykola Seredych,[4] Teresa J. Bandosz,[4] and Robert Alfano[1,2,*]

[1]*Department of Electrical Engineering, The City College of New York, 160 Convent Avenue, New York 10031, USA*

[2]*IUSL, Department of Physics, The City College of New York, 160 Convent Avenue, New York 10031, USA*

[3]*Department of Bio-medical Engineering, The City College of New York, 160 Convent Avenue, New York 10031, USA*

[4]*Department of Chemistry, The City College of New York, 160 Convent Avenue, New York 10031, USA*

**Corresponding author: ralfano@sci.ccny.cuny.edu*

Received December 4, 2012; revised February 14, 2013; accepted February 14, 2013;
posted February 15, 2013 (Doc. ID 180995); published March 14, 2013

The optical properties of zinc (hydr)oxide and its porous composites with 2% and 5% graphite oxide (GO), thus forming ZnGO-2 and ZnGO-5, are investigated using reflectance spectroscopy and two-photon fluorescence (TPF) imaging. The bandgap energies for the $Zn(OH)_2$, ZnGO-2, and ZnGO-5 samples are determined to be in the range between 2.88 and 3.60 eV. The size of light-emitting regions (~from 4.5 to 45 μm) and pore size (~from 20 to 255 μm) are measured using the TPF imaging technique.

OCIS codes: 160.0160, 160.4236, 300.0300, 300.6170.

The subject of energy band structures and critical points of porous microcomposites has attained renewed interest because of the potential applications of these new optical materials in sensors and solar energy convertors [1,2]. The determination of the optical bandgap energies and transitions between critical points (i.e., between valence and conduction bands) are important because they not only control the efficiency for solar conversion and the shape of the optical emission spectrum, but also manifest the effect of structural and thermal disorder on the electronic properties of the composite materials [3]. Direct interband transitions are believed to be responsible for the peaks observed in the derivative of reflectivity with respect to energy of a number of semiconductors and composite materials in the spectral energy range between 1 and 12 eV [4]. Identification of these critical points would provide insight into the band structure of these materials over a wide spectral range of energies, as indicated in [4]. Wavelength modulation techniques using derivatives of normalized reflectance spectra [i.e., $(1/R)(dR/dE)$] and two-photon fluorescence (TPF) imaging techniques have been identified as two most robust methods in the measurement and analysis of bandgap energies and porous and light-emitting regions.

In this Letter, the first-order derivative of reflectance, a modulation technique, as a function of photon energy has been employed to determine the bandgaps and critical transition energies for $Zn(OH)_2$, and its composites with 2% and 5% graphite oxide (GO) as zinc-graphite oxides (referred to as ZnGO-2 and ZnGO-5, respectively). The TPF imaging technique has been used to locate the light-emitting regions and determine the sizes of pores.

Using reflectance spectroscopy GaAs, $Zn(OH)_2$, ZnGO-2, and ZnGO-5 were studied in the energy range from 1.0 to 6.1 eV. The bandgaps for ZnO and GO are reported to be 3.3 [5] and 2.4 eV [6], respectively. The reflectance spectroscopy method has proven to be efficient, as no perturbation is necessary. The interpretation of data poses no ambiguity, but it demands careful elimination of background contributions and the sensitivity of the spectrometer needs to be maintained at a value of $\Delta R/R \geq 10^{-4}$. Using the energy derivative of normalized reflectance data, effects of surface conditions on reflectance measurements are greatly minimized. The reflectance data were obtained at room temperature.

Two-photon excitation microscopy is a fluorescence imaging technique that allows imaging up to a depth of approximately 1 mm. The application of two-photon excitation fluorescence microscopy has become a powerful tool for studying biological functions in live tissues and offers many advantages over conventional imaging techniques. TPF is a technique in which a fluorophor is excited by the simultaneous absorption of two photons. The familiar one-photon fluorescence process involves exciting a fluorophor from the electronic ground state to an excited state by a single photon. This process typically requires photons in the ultraviolet or blue/green spectral range. However, the same excitation process can be generated by the simultaneous absorption of two less energetic photons (typically in the infrared spectral range) under sufficiently intense femtosecond pulse laser illumination [7]. TPF imaging identifies light-emitting regions. It also identifies the pores and void regions of samples. Using this imaging technique, particle size and distribution can be estimated.

Samples of $Zn(OH)_2$, ZnGO-2, and ZnGO-5 have been investigated. GaAs served as a reference sample. ZnGO-2 and ZnGO-5 samples were prepared by synthesis of $Zn(OH)_2$ doped with 2% and 5% GO following reference [2]. GO was synthesized by oxidation of graphite (Sigma-Aldrich) using the Hummers method [8]. The composites were prepared by dispersing GO powder (2 or 5 wt. %) of the final mass of the material in 1.0 L zinc chloride solution (0.05 M). The resulting well-dispersed suspension was stirred for 4 h. Hydr(oxide) solution (0.05 M) was then added (2.0 L) at a rate of 2.0 mL per min using a Titronic Universal. Afterward, the obtained composites were extensively washed with distilled water until neutral pH was achieved and no traces of chloride ions were found. The suspension was centrifuged and a formed gel was dried at 100°C over 48 h. Zinc (hydr)oxide was

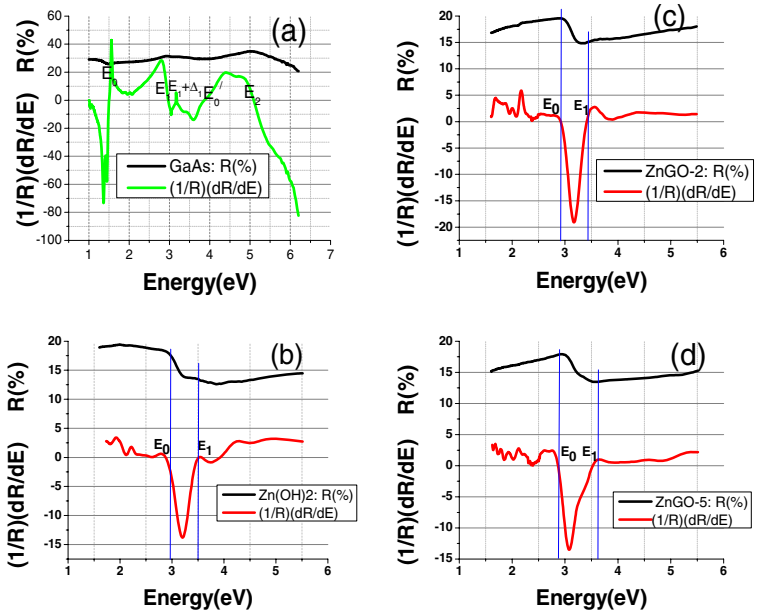

Fig. 1. (Color online) Reflectance spectra and their derivatives were used for determining the critical point energies for different materials: (a) GaAs, (b) porous $Zn(OH)_2$, (c) ZnGO-2, and (d) ZnGO-5. For clarity, two vertical lines that intersect the derivative curves at locations, identified as $E_0 = E_g$ and E_1, are shown in Figs. 1(b)–1(d).

prepared in the same way, without the GO in $ZnCl_2$ solutions. Some details on $Zn(OH)_2$ are discussed in [2]. The samples were characterized at room temperature by reflectance spectroscopy (Varian's Cary 500 Scan-Spectro-Photometer) between the spectral UV and NIR ranges. The samples were dispersed in deionized water with a fixed concentration (5 mg/4 ml) [2]. The samples used for reflectance and TPF imaging were all 8 mm in diameter and of 150 μm thickness. The device used to measure the reflectance spectra was designed to calculate absolute reflectance using a pair of matched mirrors as comparison mirrors to perform the calibration and measure the sample's reflectance.

The reflectance spectra and their derivatives for three samples, $Zn(OH)_2$, ZnGO-2, and ZnGO-5 shown in Figs. 1(b)–1(d), are very much alike, reflecting the similarity of their band structures. Similar groups in different semiconductors or materials are believed to come from transitions in the similar general areas of the band structures. The bandgap energies of the three samples $Zn(OH)_2$, ZnGO-2, and ZnGO-5 have been labeled with E_0 and E_1 only. Critical points of transition that have been labeled as E_0, $E_0 + \Delta_0$, E_1, $E_1 + \Delta_1$, E_0', and E_2 were obtained using $(1/R)dR/dE = 0$ for GaAs in [9] and are compared with results reported in [9]. The critical point at E_0 (i.e., E_g) is identified as the direct bandgap energy, while the critical point at $E_0 + \Delta_0$ corresponds to a transition from the split-off valence band at $k = 0$, which arises through the spin orbit interaction. The transitions at E_1 and $E_1 + \Delta_1$ corresponding to Λ-point and L-point transitions are also due to spin-orbit splitting. Although the detailed band structure and notation given to GaAs are obtained from [9], the values of pertinent interband transitions are given in Table 1 for GaAs (as a reference), $Zn(OH)_2$, ZnGO-2, and ZnGO-5.

TPF imaging was performed with the Ultima Multi-Photon-Microscope (Olympus BX-51 of Prairie Tech. Inc., WI, USA). An excitation energy between 1.82 eV (680 nm) and 1.15 eV (1080 nm) was used to conduct TPF imaging. The samples, in particular, were excited with 100 fs laser pulses with an energy of 1.569 eV (i.e., 790 nm) using the Ti-sapphire (Chameleon Ultra II laser, Coherent Inc.) laser, and the fluorescence emitted from the specimen was collected by the photomultiplier tubes after passing barrier filters (450–490 nm).

The two-dimensional (2D) images (239.1 μm × 239.1 μm) produced on the screen (512 × 512 pixels) were recorded, as shown in Fig. 2. For 3D images, we collected Z-series image stacks with defined ranges for the start position, stop position, and step size.

The image stacks were analyzed using Image J software (National Institutes of Health). After importing images into image J, image properties of pixel width

Table 1. Critical Point Energies (eV) of a Few Materials

Materials	Previous Results (eV)	Present Results (eV)
GaAs	$E_0 = 1.5192^a$	$E_0 = E_g = 1.50$
	$E_0 + \Delta_0 = 1.859^a$	
	$E_1 = 3.017^a$	$E_1 = 2.99$
	$E_1 + \Delta_1 = 3.245^a$	$E_1 + \Delta_1 = 3.20$
	$E_0' = 3.8^b$	$E_0' = 3.80$
	$E_1' + \Delta_1' = 4.659^a$	
	$E_2 = 5.11^a$	$E_2 = 5.11$
$Zn(OH)_2$	$E_0 = E_g = 2.97^c$	$E_0 = E_g = 2.98$
		$E_1 = 3.5$
ZnGO-2	$E_0 = E_g = 2.93^c$	$E_0 = E_g = 2.90$
		$E_1 = 3.40$
ZnGO-5	$E_0 = E_g = 2.84^c$	$E_0 = E_g = 2.88$
		$E_1 = 3.60$

[a]Ref. [9], measured at 4K.
[b]Ref. [4].
[c]Measured by us from absorption edge at room temperature.

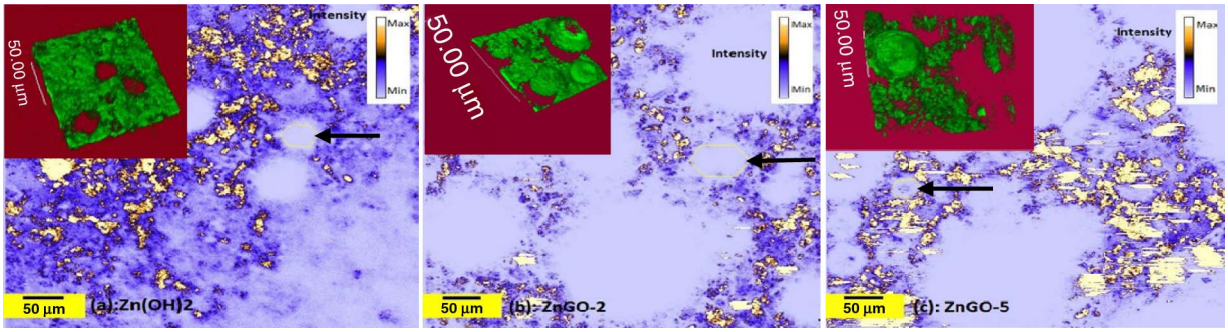

Fig. 2. (Color online) TPF images showing voids and light-emitting regions: (a) A 2D image for $Zn(OH)_2$ with the pore size ranging from 20 to 63 μm, (b) A 2D image for ZnGO-2 with the pore size ranging from 25 to 255 μm, and (c) A 2D image for ZnGO-5 with pore size ranging from 20 to 232 μm. A 3D image for each sample is shown in the insets on the upper-left corner of each figure. Upper-right corner of images show intensity bars of emitted regions of samples, where white color denotes region of maximum emitted light whereas light blue color denotes region of no light. The arrows shown in (a)–(c) show that the holes are almost hexagonal in shape.

(0.467 μm) and height (0.467 μm) in the X and Y directions, and voxel depth (1 μm) in the Z direction were provided. They were then converted into 8 bit images to reconstruct the 3D images. The clearest images were chosen for analysis.

TPF images shown in Figs. 2(a)–2(c) are very similar. These three samples indicate the presence of holes between the aggregates of particles. These holes are almost hexagonal in shape, and these three images also show light-emitting regions that are nothing but the aggregates of nanoparticles. Particle size distribution of luminscent average area of $Zn(OH)_2$, ZnGO-2, and ZnGO-5 were 143 μm^2 [av. size, $\sim(11.94 \pm 3.21)$ μm, min 4.5 μm, max 17.0 μm], 318 μm^2 [av. size, $\sim(17.83 \pm 4.52)$ μm, min 4.5 μm, max 21.0 μm], 551 μm^2 [av. size, $\sim(23.48 \pm 5.18)$ μm, min 5.0 μm, max 45.0 μm], and area of pores 498 μm^2 [min 20.0 μm, max 63.0 μm diameter], 982 μm^2 [min 25.0 μm, max 255.0 μm diameter], and 827 μm^2 [min 20.0 μm, max 232.0 μm diameter], respectively.

In these composite materials, ZnGO-2 and ZnGO-5, the particles of the inorganic phases are smaller in size than those in the parent material $Zn(OH)_2$ and they are clearly seen in Figs. 2(b) and 2(c) as they are deposited on the graphene sheet as a thin layer. The measured surface areas of $Zn(OH)_2$, ZnGO-2, and ZnGO-5 are 72, 64, and 64 m^2/g, respectively, and the total pore volume increases with an increase in the amount of GO present in the composites. The bandgap and critical points of transition for a new class of optical microcomposite materials (ZnGO-2 and ZnGO-5) have been investigated using reflectance spectroscopy and the derivatives of such data. The TPF imaging technique reported herein for the first time in investigating these composite materials, ZnGO-2 and ZnGO-5, show the presence of voids and their increase in size as the percent of GO increases in the composites. The light-emitting regions, observed via TPF imaging technique, that are aggregates of microparticles vary in size in the studied samples and this unique imaging technique shows the structural details of the composites that are reported for the first time. The current studies on these microcomposites have proven to be very useful as $Zn(OH)_2$, ZnGO-2, and ZnGO-5 hold promise as new materials for their unique capacities in harvesting solar energy and their storage purposes. The pore sizes are possibly suitable for doping with dye molecules and quantum dots to enhance solar conversion.

This work was supported in part by the army research grant W911NF-10-1-0030 and NSF collaborate grant 1133112.

References

1. J. T. Robinson, F. K. Perkins, E. S. Snow, Z. Wei, and P. E. Sheenhan, Nano Lett. **8**, 3137 (2008).
2. M. Seredych, O. Mabayoje, M. M. Kolesnik, V. Krstic, and T. J. Bandosz, J. Mater. Chem. **22**, 7970 (2012).
3. S. R. Johnson and T. Tiedje, J. Appl. Phys. **78**, 5609 (1995).
4. H. Ehrenreich, H. R. Philipp, and J. C. Phillips, Phys. Rev. Lett. **8**, 59 (1962).
5. S. Venkataprasad Bhat and F. L. Deepak, Solid State Commun. **135**, 345 (2005).
6. H. K. Jeong, M. H. Jin, K. P. So, S. C. Lim, and Y. H. Lee, J. Phys. D **42**, 065148 (2009).
7. J. Bewersdorf, P. Rainer, and S. W. Hell, Opt. Lett. **23**, 655 (1998).
8. W. S. Hummers and R. E. Offeman, J. Am. Chem. Soc. **80**, 1339 (1958).
9. P. Y. Yu and M. Cardona, *Fundamentals of Semiconductors: Physics and Materials Properties*, 4th ed. (Springer, 2010); fig 16.41 a/b on p. 306, and Table 6.3 on p. 258.